Central European Journal of Physics 9 (2011) 432-437.

ELECTRONIC EXCITATIONS IN $ZnWO_4$ AND $Zn_xNi_{1-x}WO_4$ (x=0.1-0.9) USING VUV SYNCHROTRON RADIATION

Aleksandr Kalinko[1], Alexey Kotlov[2], Alexei Kuzmin[1†], Vladimir Pankratov[1], Anatoli I. Popov[1,3], Liana Shirmane[1]

[1] Institute of Solid State Physics, University of Latvia,
Kengaraga street 8, LV-1063, Riga, Latvia
[2] Hamburger Synchrotronstrahlungslabor HASYLAB at Deutsches
Elektronensynchrotron DESY, Notkestraβe 85, Hamburg 22607, Germany
[3] Institute Laue Langevin, 6 rue Jule Horovitz, 38042, Grenoble, France

Abstract: The photoluminescence spectra and luminescence excitation spectra of pure microcrystalline and nano-sized $ZnWO_4$ as well as the $Zn_xNi_{1-x}WO_4$ solid solutions were studied using vacuum ultraviolet (VUV) synchrotron radiation. The samples were also characterized by x-ray powder diffraction. We found that: (i) the shape of the photoluminescence band at 2.5 eV, being due to radiative electron transitions within the $[WO_6]^{6-}$ anions, becomes modulated by the optical absorption of Ni^{2+} ions in the $Zn_xNi_{1-x}WO_4$ solid solutions; and (ii) no significant change in the excitation spectra of $Zn_{0.9}Ni_{0.1}WO_4$ is observed compared to pure $ZnWO_4$. At the same time, a shift of the excitonic bands to smaller energies and a set of peaks, attributed to the one-electron transitions from the top of the valence band to quasi-localized states, were observed in the excitation spectrum of nano-sized $ZnWO_4$.

PACS (2008): 78.55.Hx, 81.07.Wx, 71.35.-y

Keywords:
$ZnWO_4$ • $Zn_xNi_{1-x}WO_4$ solid solutions • tungstates • electronic excitations • luminescence • VUV spectroscopy

† E-mail: a.kuzmin@cfi.lu.lv

1. Introduction

Sanmartinite ($ZnWO_4$) belongs to a wide group of wolframite-type tungstates having the general formula AWO_4 with A^{2+}= Mg^{2+}, Mn^{2+}, Fe^{2+}, Co^{2+}, Ni^{2+}, Zn^{2+}, and Cd^{2+} [1]. It is a technologically important material, which finds applications such as scintillation detectors, laser-active hosts, optical fibers, sensors, and phase-change optical recording media [2, 3, 4, 5, 6, 7]. In addition, $ZnWO_4$ shows highly efficient (>50%) picosecond multiple Stokes and anti-Stokes generation when used as a Raman-active crystal in solid-state lasers, based on stimulated Raman scattering (SRS) [5, 8]. In the latter case, the strong SRS-active Raman mode at 907 cm^{-1} is the internal stretching W-O A_g-mode in the WO_6 octahedra [5, 8]. The tuning of the mode frequency can be achieved in tungstate solid solutions. Three such systems are known based on zinc tungstate: $ZnWO_4$-$FeWO_4$ [9], $ZnWO_4$-$MnWO_4$ [9], and $ZnWO_4$-$NiWO_4$ [10]. The latter system finds also application as a yellow ceramic pigment [10].

The optical and luminescent properties of wolframite-type $ZnWO_4$ have been widely studied in the past more than once. In particular, the intrinsic luminescence band, observed at room temperature at about 2.5 eV, has been attributed to a charge transfer between oxygen and tungsten ions in the $[WO_6]^{6-}$ anions [11-14]. The contributions from defects and distorted tungsten-oxygen octahedra have been also observed [15-17]. Up to now, most fundamental studies on tungstates have been performed on single-crystal samples. In this work we present the results on nano-sized $ZnWO_4$ and microcrystalline $Zn_xNi_{1-x}WO_4$ solid solutions using vacuum ultraviolet (VUV) synchrotron radiation spectroscopy.

2. Experiment

Pure $ZnWO_4$ and the solid solutions $Zn_xNi_{1-x}WO_4$ (x=0.1-0.9) were synthesized using a co-precipitation technique [18, 19]. All chemicals used were analytic grade reagents (purity 99%, “Reahim”) without further purification. Pure $ZnWO_4$ was prepared by the reaction of $ZnSO_4 \cdot 7H_2O$ and $Na_2WO_4 \cdot 2H_2O$ at room temperature (20ºC), pH 8, and a reaction time of 1-2 hours. The water solutions of the two salts were prepared by dissolving 10 mmol of the salt in 100 ml of double-distilled water with vigorous stirring. Next they were mixed in 1:1 molar ratio, and white precipitates appeared immediately. After completion of the precipitate reaction, the precipitate

was filtered off, washed several times with distilled water, and dried in air for 12 hours at 80ºC thus resulting in the white-colored nano-sized $ZnWO_4$ powder [19]. Previous structural studies indicated that the $ZnWO_4$ powder as prepared has particles of size below 2 nm and a relaxed $ZnWO_4$ structure [19, 20].

The nano-sized powder was next annealed in air for 4 hours at 400ºC and 800ºC. Annealing above 400ºC results in the growth of crystallites, so that material becomes microcrystalline [19]. The yellow-colored solid solutions $Zn_xNi_{1-x}WO_4$ (x=0.1-0.9) were prepared by first mixing proper amounts of water solutions of $ZnSO_4 \cdot 7H_2O$ and $Ni(NO_3)_2 \cdot 6H_2O$ salts and further following the same preparation procedure. After drying, the obtained solid solutions were annealed in air for 4 hours at 800ºC.

The samples' crystallinity and phase composition (formation of solid solution) were controlled by x-ray powder diffraction (XRD). The XRD patterns (Fig.1) were recorded at 20°C using a Bragg-Brentano powder diffractometer with a graphite monochromator in the diffracted beam to eliminate the specimen's fluorescence. A conventional tube with a copper anode (Cu $K\alpha$ radiation) was used as x-ray source. The measurements were performed in the angle range 2θ=5-70° with the step $\Delta(2\theta)$=0.05°. The XRD data (ICSD No. 81937) for monoclinic ($P2/c$) $ZnWO_4$ from [21] were used for comparison.

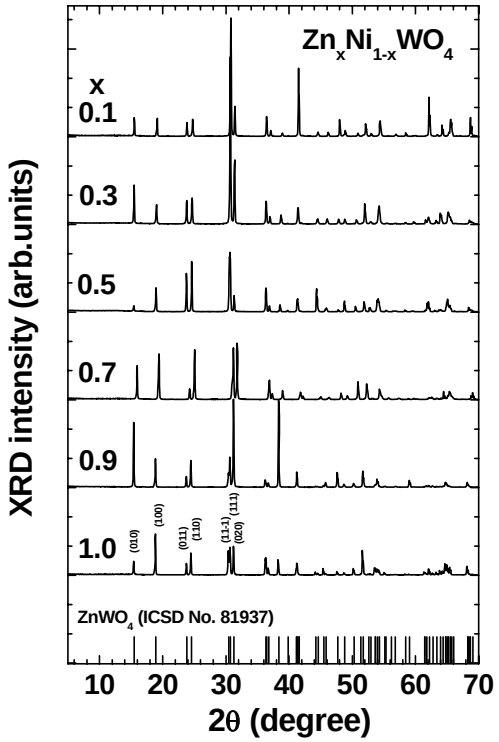

Figure 1. X-ray diffraction patterns of the microcrystalline $ZnWO_4$ and $Zn_xNi_{1-x}WO_4$ solid solutions annealed at 800ºC. (Only a few patterns are shown for clarity).

The photoluminescence spectra were measured using pulsed YAG:Nd laser excitation (4.66 eV, 8 ns) at 20ºC. The excitation spectra were collected at room temperature exploiting ultraviolet (UV) and vacuum ultraviolet (VUV) synchrotron radiation (3.6–20 eV) emitted from the DORIS III storage ring at the SUPERLUMI station (HASYLAB DESY, Hamburg). The measurement procedure has been described in details elsewhere [22, 23].

Table 1. Lattice parameters (*a*, *b*, *c*, *β*) and unit cell volume (*V*) of monoclinic (*P*2/*c*) $ZnWO_4$ (x=1) and $Zn_xNi_{1-x}WO_4$ (x=0.1-0.9) solid solutions annealed at 800ºC.

x	*a* (Å)	*b* (Å)	*c* (Å)	*β* (º)	*V* (Å^3)
1	4.69	5.72	4.93	90.7	132.4
0.9	4.69	5.73	4.94	90.5	132.9
0.8	4.67	5.69	4.93	90.3	131.1
0.7	4.67	5.70	4.92	90.4	130.9
0.6	4.68	5.70	4.94	90.5	131.5
0.5	4.66	5.70	4.93	90.2	131.1
0.4	4.65	5.70	4.93	90.0	130.7
0.3	4.64	5.69	4.93	90.1	130.3
0.1	4.61	5.68	4.92	90.0	129.0

3. Results and discussion

The XRD patterns in Fig. 1 indicate that pure $ZnWO_4$ and the $Zn_xNi_{1-x}WO_4$ solid solutions are formed after annealing at 800ºC. The XRD pattern of pure $ZnWO_4$ was indexed using the standard data (Inorganic Crystal Structure Database (ICSD) No. 81937) for monoclinic (*P*2/*c*) $ZnWO_4$ from [21]. Upon substitution of Zn^{2+} by Ni^{2+} ions, the positions of the Bragg peaks in the XRD patterns shift slightly in the direction of larger scattering angles for increasing nickel content due to a decrease of the lattice parameters (Table 1). Upon increasing nickel content (x), the variation of the *c* parameter is small (~0.01 Å), but the values of the *a* and *b* parameters decrease by ~0.08 Å and ~0.04 Å, respectively. Also the unit cell volume decreases from *V* =132.4 Å^3 in $ZnWO_4$ to *V* =129.0 Å^3 in $Zn_{0.1}Ni_{0.9}WO_4$. The results reported in Table 1 are in agreement with that found in the literature for pure tungstates ($ZnWO_4$ [10, 21] and $NiWO_4$ [24]) and $Zn_xNi_{1-x}WO_4$ solid solutions [10]. Note that the unit cell

volume in $NiWO_4$ (V=127.7 Å^3) [24] is expected to be smaller by only about 3.5% than that of $ZnWO_4$ (V=132.3 Å^3) [21].

The phase of the $Zn_xNi_{1-x}WO_4$ solid solutions remains monoclinic wolframite-type, and the appearance of any other phases was not observed, in agreement with [10]. Such behaviour can be expected from the close size of Zn^{2+} and Ni^{2+} ions [25] and is in agreement with previous findings in [10]. Note that the Bragg peaks in the XRD patterns in Fig. 1, for example, the three Bragg peaks (11-1), (111), and (020) located at 2θ=31º, are slightly better resolved than in [10].

The photoluminescence spectrum of pure $ZnWO_4$ powder consists of a broad band, peaked at about 2.5 eV (Fig. 2). When mixed with $NiWO_4$, the $Zn_xNi_{1-x}WO_4$ solid solutions are readily formed, and the luminescence spectrum splits into three sub-bands, centred at ~2.26 eV, ~2.5 eV, and ~3.0 eV. Note that the photoluminescence spectra in Fig. 2 have been normalized at the band maximum, and their intensity should not be compared. In fact, addition of nickel results in a reduction of the total photoluminescence signal. We believe that the photoluminescence in the solid solutions has origin similar to that in pure $ZnWO_4$, however it is modulated by the self-absorption effect due to the presence of the Ni^{2+} ions.

In pure $ZnWO_4$ the origin of the main band at 2.5 eV has been previously assigned to radiative electron transitions within the $[WO_6]^{6-}$ anions [11, 12]. At the same time, the band at ~2.3 eV has been attributed to recombination of e–h pairs localized at oxygen-atom-deficient tungstate ions [15, 16] or distorted WO_6 octahedra [17].

The origin of the last band at 3.0 eV appearing in the solid solutions is attributed to the interference between the broad luminescence band of the WO_6 groups and the absorption band of the NiO_6 groups. The self-absorption effect is caused by the intensive transition at ~2.72 eV from the ground state $^3A_{2g}$ to the excited state $^3T_1$ of Ni^{2+} ($3d^8$) ions [10, 26] in distorted octahedral coordination [24]. The presence of this absorption band results in a notch at 2.7 eV in the emission band, thus making the peak at ~3.0 eV more pronounced.

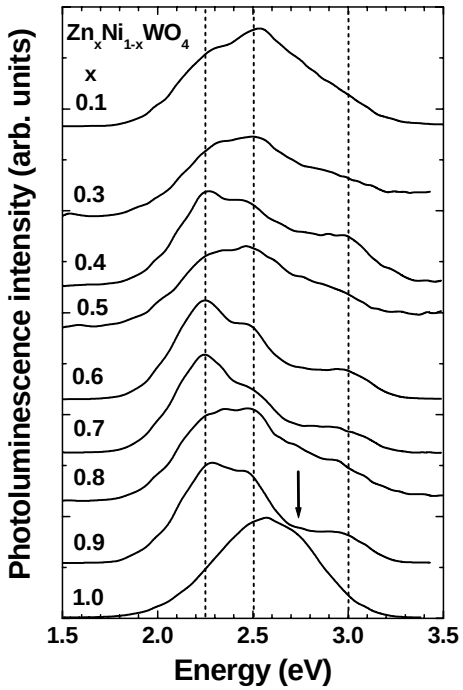

Figure 2. Photoluminescence of microcrystalline pure $ZnWO_4$ (x=1) and the $Zn_xNi_{1-x}WO_4$ solid solutions annealed at 800°C.

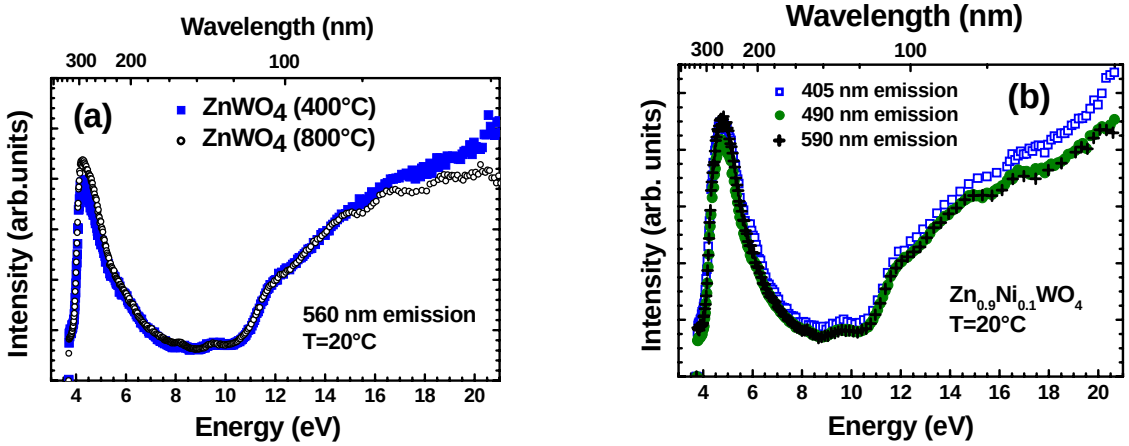

Figure 3. Room temperature (20ºC) excitation spectra of pure $ZnWO_4$ and $Zn_{0.9}Ni_{0.1}WO_4$. (a) 560 nm emission in pure $ZnWO_4$, obtained from nano-sized $ZnWO_4$ by annealing at 400ºC (solid squares) and 800ºC (open circles). (b) 405 nm (open squares), 490 nm (solid circles) and 590 nm (crosses) emission in $Zn_{0.9}Ni_{0.1}WO_4$.

The excitation spectra are similar for pure $ZnWO_4$ and 10% Ni-doped $ZnWO_4$ powders (Fig. 3). They consists of a strong band at ~4.0 eV having the excitonic origin [11, 12]. The intensity of the excitation spectra starts to grow in the energy

region above ~11 eV due to the beginning of the multiplication of electronic excitation (MEE) process [11, 12]. In this process, a secondary electron–hole (e–h) pair is created due to the inelastic scattering of a sufficiently 'hot' photoelectron, having an energy exceeding twice that of the band gap value. Further increase of the excitation energy results in deeper valence electrons starting to participate in the MEE process. Finally, when the photon energy reaches ~17 eV, i.e., $\approx 2E_g+E_V$ where $E_g \approx$ 4.6-4.9 eV is the band gap energy [11, 27, 28], and $E_V \approx$ 7.5 eV (Fig. 5) is the valence band width [28], the electrons from the bottom of the valence band participate in the MEE process, and the intensity of the excitation spectra exhausts [11, 12]. Note also that the excitation spectra in Fig. 3 are weakly modulated by a fine structure giving rise to several peaks at about 6, 8, 9.5, 12, 15, and 17 eV: among these the last four peaks are better visible. These energies correlate with the one-electron transitions from the top of the valence band to the conduction band as supported by our LCAO (linear combination of atomic orbitals) calculations [28].

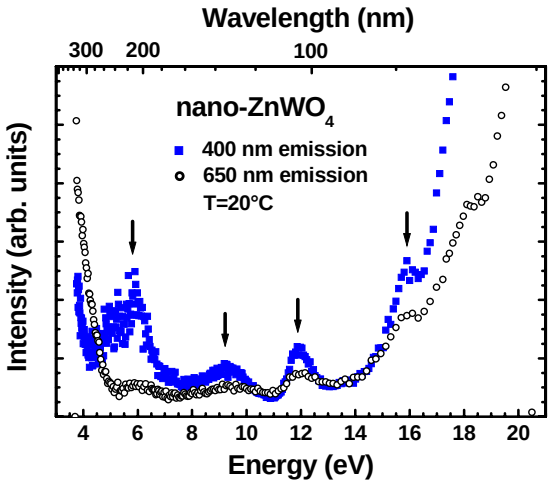

Figure 4. Room temperature (20ºC) excitation spectra of the 400 nm and 650 nm emissions in pure as-prepared nano-sized $ZnWO_4$, dried in air for 12 hours at 80ºC. The bands due to one-electron transitions are indicated by vertical arrows.

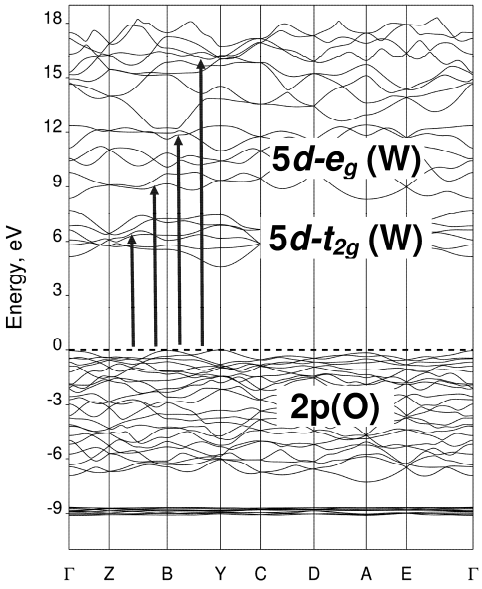

Figure 5. Band structure diagram for wolframite-type $ZnWO_4$ from [28]. The energy zero is set at the Fermi energy level. The one-electron transitions, corresponding to the peaks (see Fig. 4) in the excitation spectra of nano-sized $ZnWO_4$, are indicated by vertical arrows.

The excitation spectra in nano-$ZnWO_4$ detected at 400 nm and 650 nm, are close to that from the crystal (Fig. 4). However, a strong band of the excitonic origin is shifted to smaller energies below ~4.0 eV, due to a decrease of the optical band gap caused by disorder [29]. The presence of local structural relaxation in nano-$ZnWO_4$ is confirmed by the extended x-ray absorption fine structure (EXAFS) studies [20] and is in agreement with the recent Raman and luminescence results [19]. A set of peaks observed at 6, 9, 12, and 16 eV in Fig. 4 is attributed to the one-electron transitions from the top of the valence band to quasi-localized states. Such interpretation is in agreement with the first principles LCAO calculations [28] of the band structure for wolframite-type $ZnWO_4$ (Fig. 5). The LCAO calculations show that the valence band of $ZnWO_4$, having largely O 2p character, is separated by the band gap of 4.6 eV from the bottom of conduction band, which is dominated by W 5d states [28]. Therefore, the peaks located between 5 eV and 17 eV in excitation spectra of nano-$ZnWO_4$ (Fig. 4) are of charge transfer type from oxygen to tungsten.

4. Conclusions

The luminescence spectra and luminescence excitation spectra of pure microcrystalline and nano-sized $ZnWO_4$ and the $Zn_xNi_{1-x}WO_4$ solid solutions were studied using vacuum ultraviolet (VUV) synchrotron radiation.

The addition of nickel to $ZnWO_4$ increases the intensity of emission at ~2.3 eV due to a distortion of WO_6 octahedra. The excitation spectra are similar in pure and $Zn_{0.9}Ni_{0.1}WO_4$ powders showing strong excitonic band at ~4.0 eV and the effect from multiplication of electronic excitation (MEE) process above ~11 eV.

The shift of the excitonic band in the excitation spectra of nanosized $ZnWO_4$ is caused by the local structural relaxation. In nanosized $ZnWO_4$, a number of bands is observed in the excitation spectra due to one-electron transitions from the top of the valence band to quasi-localized states.

Acknowledgements

This work was supported by ESF Project 2009/0202/1DP/1.1.1.2.0/09/APIA/VIAA/141, Latvian Government Research Grant No. 09.1518 and Joint Project No. 10.0032. The research leading to these results has also received funding from the European Community's Seventh Framework Programme (FP7/2007-2013) under grant agreement No. 226716.

References

[1] A. W. Sleight, Acta. Cryst. B 28, 2899 (1972)

[2] H. Wang, F. D. Medina, D. D. Liu, Y. D. Zhou, J. Phys: Condensed Matter 6, 5373 (1994)

[3] H. Kraus, V. B. Mikhailik, Y. Ramachers, D. Day, K.B. Hutton, J. Telfer, Phys. Lett. B 610, 37 (2005)

[4] H. Grassmann, H. G. Moser, E. Lorenz, J. Lumin. 33, 21 (1985)

[5] A. A. Kaminskii, H. J. Eichler, K. Ueda, N. V. Klassen, B. S. Redkin, L. E. Li, J. Findeisen, D. Jaque, J. Garcia-Sole, J. Fernandez, R. Balda, Applied Optics 38, 4533 (1999)

[6] A. R. Phani, M. Passacantando, L. Lozzi, S. Santucci, J. Mater. Sci. 35, 4879 (2000)

[7] A. Kuzmin, R. Kalendarev, A. Kursitis, J. Purans, J. Non-Cryst. Solids 353, 1840 (2007)

[8] H. M. Pask, Prog. Quant. Electron. 27, 3 (2003)

[9] L. C. Hsu, Am. Mineral. 66, 298 (1981)

[10] A. L. M. de Oliveira, J. M. Ferreira, M. R. S. Silva, G. S. Braga, L. E. B. Soledade, M. A. M. M. Aldeiza, C. A. Paskocimas, S. J. G. Lima, E. Longo, A. G. Souza, I. M. G. Santos, Dyes and Pigments 77, 210 (2008)

[11] V. N. Kolobanov, I. A. Kamenskikh, V. V. Mikhailin, I. N. Shpinkov, D. A. Spassky, B. I. Zadneprovsky, L. I. Potkin, G. Zimmerer, Nucl. Instrum. and Methods in Phys. Res. A 486, 496 (2002)

[12] V. Nagirnyi, E. Feldbach, L. Jonsson, M. Kirm, A. Kotlov, A. Lushchik, V. A. Nefedov, B. I. Zadneprovski, Nucl. Instrum. and Methods in Phys. Res. A 486, 395 (2002)

[13] V. Pankratov, L. Grigorjeva, D. Millers, S. Chernov, S. Voloshinovskii, J. Lumin. 94, 427 (2001)

[14] L. Grigorjeva, D. Millers, S. Chernov, V. Pankratov, A. Watterich, Rad. Measurements 33, 645 (2001)

[15] M. Itoh, T. Katagiri, T. Aoki, M. Fujita, Rad. Measurements 42, 545 (2007)

[16] Z. Lou, J. Hao, M. Cocivera, J. Lumin. 99, 349 (2002)

[17] V. B. Mikhailik, H. Kraus, G. Miller, M. S. Mykhaylyk, D. Wahl, J. Appl. Phys. 97, 083523 (2005)

[18] G. Huang, Y. Zhu, Mater. Sci. Eng. B 139, 201 (2007)

[19] A. Kalinko, A. Kuzmin, J. Lumin. 129, 1144 (2009)

[20] A. Kuzmin, A. Kalinko, J. Timoshenko, HASYLAB Annual Report 2009: http://hasylab.desy.de/annual_report/files/2009/2009560.pdf

[21] P. F. Schofield, K. S. Knight, G. Cressey, J. Mater. Sci. 31, 2873 (1996)

[22] G. Zimmerer, Rad. Measurements 42, 859 (2007)

[23] V. Pankratov, M. Kirm, H. von Seggern, J. Lumin. 113, 143 (2005)

[24] H. Weitzel, Z. für Kristallographie 144, 238 (1976)

[25] R. D. Shannon, Acta Cryst. A 32, 751 (1976)

[26] L. N. Limarenko, A. E. Nosenko, M. V. Pashkovskii, D.-L. L. Futorskii, Influence of structural defects on physical properties of tungstates (Vysha Shkola, Lvov:, 1978)

[27] M. Itoh, N. Fujita, Y. Inabe, J. Phys. Soc. Jap. 75, 084705 (2006)

[28] A. Kalinko, A. Kuzmin, R. A. Evarestov, Solid State Commun. 149, 425 (2009)

[29] E. Orhan, M. Anicete-Santos, M. A. M. A. Maurera, F. M. Pontes, A. G. Souza, J. Andrés, A. Beltrán, J. A. Varela, P. S. Pizani, C. A. Taft, E. Longo, J. Solid State Chem. 178, 1284 (2005)